FEM Simulations of the Effects of Fouling Deposits on Laser-Generated Lamb Waves

Suorsa, Joonas Fredrik

IEEE
2022-10

Suorsa , J F , Mustonen , J A , Iablonskyi , D , Klami , A , Salmi , A & Haeggström , E 2022 , FEM Simulations of the Effects of Fouling Deposits on Laser-Generated Lamb Waves . in 2022 IEEE International Ultrasonics Symposium (IUS) . IEEE , pp. 1-3 , 2022 IEEE International Ultrasonics Symposium (IUS) , Venice , Italy , 10/10/2022 . https://doi.org/10.1109/IUS54386.2022.995

http://hdl.handle.net/10138/352774
https://doi.org/10.1109/IUS54386.2022.9957703

submittedVersion

FEM Simulations of the Effects of Fouling Deposits on Laser-Generated Lamb Waves

Joonas Suorsa
Electronics Research Laboratory
University of Helsinki
Helsinki, Finland
joonas.suorsa@helsinki.fi

Joonas Mustonen
Electronics Research Laboratory
University of Helsinki
Helsinki, Finland
joonas.mustonen@helsinki.fi

Denys Iablonskyi
Electronics Research Laboratory
University of Helsinki
Helsinki, Finland
denys.iablonskyi@helsinki.fi

Arto Klami
Department of Computer Science
University of Helsinki
Helsinki, Finland
arto.klami@helsinki.fi

Ari Salmi
Electronics Research Laboratory
University of Helsinki
Helsinki, Finland
ari.salmi@helsinki.fi

Edward Hæggström
Electronics Research Laboratory
University of Helsinki
Helsinki, Finland
edward.haeggstrom@helsinki.fi

***Abstract*— Accumulation of fouling in industrial pipelines is a widespread and costly problem. For efficient cleaning, fouling should be quantified and located. Ultrasonic guided waves provide an efficient way to probe fouling compared to slow point-by-point measurements. Traditional methods employ transducer collars to reduce the problem to 1D, whereas our approach that employs a point excitation retains the information about the 3D geometry. By simulating fouling configurations, the effects of fouling on the ultrasound propagation in the pipe can be characterized and used for fouling quantification and localization. The results show that the most prominent effects are caused by the thickness and extent of the fouling.**

Keywords—laser-ultrasonics, guided waves, FEM, fouling detection

I. Introduction

Fouling in pipelines causes problems such as corrosion, clogging or structural damage to pipe walls in many industries. [1] This results in loss of process efficiency, which can be costly if not addressed. Many methods to detect fouling in pipes exist: ultrasonic methods [1], heat transfer mapping [2], and electrical parameter mapping [3]. An efficient method for detecting and localizing fouling can help to optimize the locations and timing of the cleaning efforts, thus reducing the machinery downtime required for the cleaning procedure.

We consider the task of fouling localization using Ultrasonic guided waves (UGWs). UGWs have been used in non-destructive testing (NDT) applications. They permit single point excitation and probing over a long distance on a pipeline, and reflections, attenuation and phase changes caused by a possible fouling layer can be picked up by the receiving transducer. Compared to traditional single-transducer probing, this is more efficient, since UGWs propagate long distances with little attenuation. Lamb waves in particular are a useful group of UGWs for investigating pipeline structures due to their characteristic dispersive behavior. UGWs are sensitive to cracks and defects in structures, and thus they may be used to detect fouling [4]. However, as fouling is a different problem from a defect, as it appears in layers of different sizes and shapes, its effects should be investigated further. Wave propagation problems for layered media have previously been solved for general cases of continuous layers e.g. by the transfer matrix method [5], but a local layer of fouling differs from this.

A finite element model (FEM) was built for a numerical study on the effects of local fouling on UGWs. The effects of different parameters of a fouling layer were investigated: fouling thickness, extent, distance from the excitation, and material stiffness. Each parameter was varied in a parametric sweep of simulations. The results provide information about the behavior of UGWs in a fouled region.

II. Methods

A. Simulation model

COMSOL Multiphysics® was used to build a 2D plate model (fig. 1), that features a steel plate (1 mm thick, 72 cm long), a water domain beneath it, and a fouling layer (36 mm wide, 2 mm thick). A custom material mimicking the elastic properties of calcium hydroxide Ca(OH)2 was used as the baseline fouling throughout the simulations. The laser excitation (energy 3.6 µJ, pulse length 60 ns) was modelled in the thermoelastic regime through the *Thermal Expansion* Multiphysics coupling, which combines *Solid Mechanics* with *Heat Transfer*. Deposited beam power was used as a boundary condition, with the approximate temporal profile of the beam, and a Gaussian spatial distribution. The excited thermal stresses then propagate through the solids, partially leaking into the water through an Acoustic-Structure boundary between the solids and water. At the edges of the geometry, low-reflecting boundary conditions are imposed

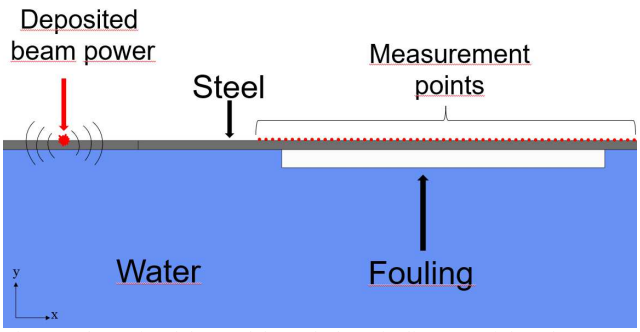

Fig. 1. Schematic of the model: steel plate, fouling material, and water. A deposited beam power boundary condition excites thermoelastic stresses in the steel, and the resulting travelling displacements are measured at the series of points. The fouling varies between 0.5λ-3.5λ in thickness and 7λ-50λ in extent compared to the A0 mode wavelength.

Funding was provided by the Academy of Finland (grant 336019).

on the steel in the x-direction, and plane wave radiation at all outer boundaries of the water domain.

B. Simulation configurations

The 2D model was chosen to ignore the circumferential wave modes arising from the pipe geometry, and isolate the fouling effects. The required computation time is also significantly shorter. Even though the simulation was done for a plate, the results generalize e.g. for a pipe with a sufficient ratio of thickness and inner radius, because the behavior of Lamb-type waves is still similar [6]. The fouling was varied by increasing its thickness and extent while keeping the other dimension constant, moving the location between the excitation and the pickup, and changing the stiffness by varying Young's modulus. Data were collected as a series of y-directional displacements at 1 mm intervals along the surface of the plate, starting from near the excitation point, the last point of the series chosen as the pickup.

C. Analysis

The displacements at the measurement points were collected into matrices with the time, and spatial indices of the points for dimensions to permit the use of 2D fast Fourier transform. The results of the sweeps were studied across the varied fouling parameters. Signals and envelopes were compared for changes in amplitude and time of flight of the first echoes, and frequency spectra for shifts in the dominant frequency. Dispersion curves were plotted from a 2D FFT of the displacements along the measurement points, and then analyzed to gain a general understanding of the effects induced by the fouling.

III. Results

The study of the fouling extent effect is shown in Fig. 2. The extent of the fouling was increased from 36 mm to 252 mm, starting from a clean plate. The time of flight of the Lamb A0 mode show the most notable change as a function of fouling length. In Fig. 2 the envelopes are plotted, showing a trend towards faster arrival of the A0 mode, indicating that a longer propagation time through the fouled region increases the apparent speed of the mode

Fig. 3 reveals a drop in the amplitude of the low-frequency components. The effects of increased fouling extent and thickness can be studied in a more general way using the simulated Lamb-type dispersion curves (Fig. 4). In the case of increased extent, the A0 mode becomes more pronounced at a low wavenumber, corresponding to the fast arrivals shown in Fig. 2. Increased fouling thickness shifts the A0 cut-off frequencies away from zero, which shows up as decreased dominant frequency amplitudes in Fig. 3.

The location of the fouling between the excitation and pickup allowed for more mode separation to take place before the fouled region. The fouling effect is less prominent in the region above 100 kHz (Fig. 5.).

The stiffness of the fouling material was varied by using different Young's moduli: 100 kPa to 48 GPa, compared to the clean signal (Fig. 5). This reduced the time-of-flight and amplitude, as the fouling stiffness was increased.

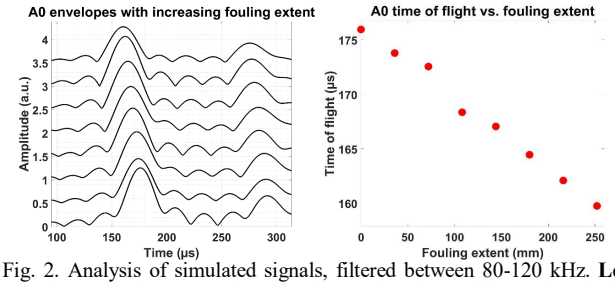

Fig. 2. Analysis of simulated signals, filtered between 80-120 kHz. **Left:** Envelopes of the A0 mode plotted as a function of increasing fouling extent, with the clean signal at the bottom. **Right:** The time of flight of the A0 mode as a function of the fouling extent.

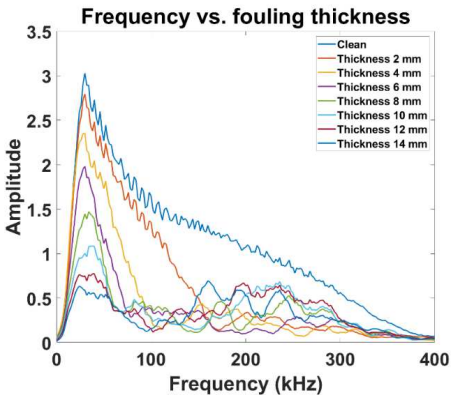

Fig. 3. The frequency spectra of the simulated signals, with the clean signal at the top. The amplitude of the dominant frequency drops as the fouling thickness was increased. A shift was also noticed in the frequencies 150-300 kHz.

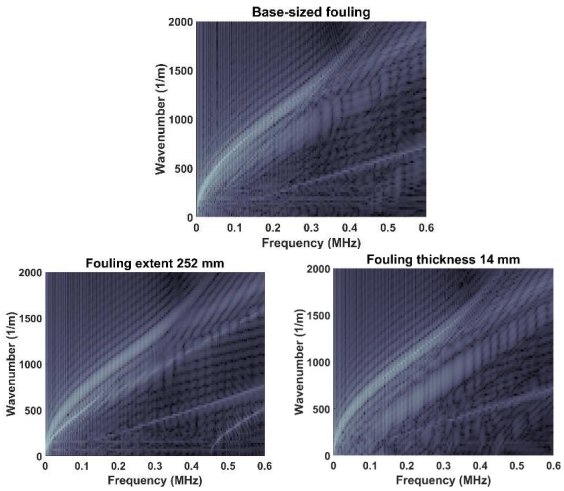

Fig. 4. Lamb-type dispersion curves of simulations with base-sized fouling (width 36 mm, thickness 2 mm), and cases where the fouling extent and thickness were increased up to seven times the base value.

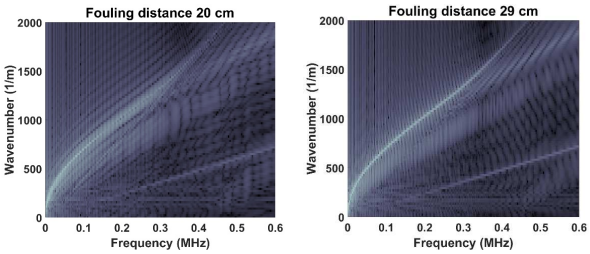

Fig. 5. Lamb-type dispersion curves of simulations with the fouling distance from the excitation point varied from 20 cm to 29 cm. As more mode separation occurs before the fouled region, the A0 mode is not affected as much as with the base distance.

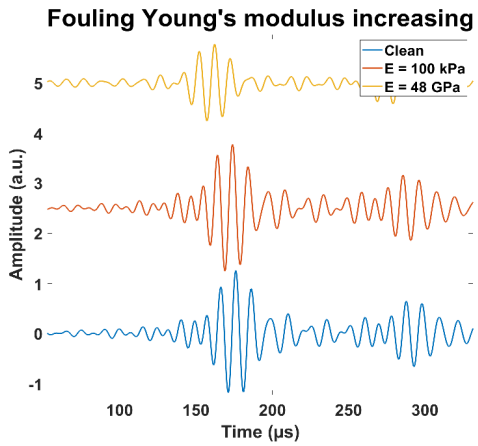

Fig. 6. Simulated signals of cases where Young's modulus of the fouling was varied. Increasing stiffness caused an amplitude drop, and a slightly faster mode arrival. Signals are offset for readability.

IV. Conclusion

Varying the properties of the fouling altered the Lamb modes. The most notable changes occurred when changing the dimensions of the fouling layer. As the extent of the fouling is increased, more time is spent on propagation through the fouled region, causing a more prominent change in the local fd-product, which resulted in time shift and a mode conversion. Fouling thickness had a greater effect on the amplitude drop of the waves. This was most notably observed in frequencies below 100 kHz. The effect of fouling distance from the transmit point was less prominent, as guided waves attenuate little. Stiff fouling affected the signals, while a low Young's modulus produced results close to those obtained without fouling. As the dimensions of the fouling batch had the most notable effects on the Lamb modes, it should be considered how different wavelengths are affected by the change.

References

[1] K. R. Lohr, J. L. Rose, "Ultrasonic guided wave and acoustic impact methods for pipe fouling detection", J. Food Eng. 56 (2003) 315–324.

[2] C. Riverol, V. Napolitano, "Estimation of fouling in a plate heat exchanger through the application of neural networks", J. Chem. Tech. 80:594–600 (2005).

[3] R. Guérin, G. Ronse, L. Bouvier, P. Debreyne, G. Delaplace, "Structure and rate of growth of whey protein deposit from in situ electrical conductivity during fouling in a plate heat exchanger", Chem. Eng. Sci. 62 (2007) pp. 1948–1957.

[4] H. Lais, P.S. Lowe, T. Gan, L.C. Wrobel, J. Kanfoud, "Characterization of the use of low frequency ultrasonic guided waves to detect Fouling deposition in pipelines", Sensors 2018, 18, 2122.

[5] L. Wang, S.I. Rokhlin, "Stable reformulation of transfer matrix method for wave propagation in layered anisotropic media", Ultrasonics 39 (2001) pp. 413-424.

[6] B. N. Pavlakovic, "Leaky guided ultrasonic waves in NDT", 1998, p. 74